Heme-Peroxidase 2, a Peroxinectin-Like Gene, Regulates Bacterial Homeostasis in *Anopheles stephensi* Midgut

Parik Kakani[1,2], Lalita Gupta[1,3] and Sanjeev Kumar[1,4]*

[1] Molecular Parasitology and Vector Biology Laboratory, Department of Biological Sciences, Birla Institute of Technology and Science (BITS), Pilani, India, [2] Department of Biological Sciences, Indian Institute of Science Education and Research (IISER), Bhopal, India, [3] Department of Zoology, Chaudhary Bansi Lal University, Bhiwani, India, [4] Department of Biotechnology, Chaudhary Bansi Lal University, Bhiwani, India

The dynamic nature of mosquito gut microbiome is associated with different stages of development and feeding behaviors. Therefore, mosquito gut harbors a wide range of endogenous microbes that promote numerous life processes such as, nutrition, reproduction and immunity. In addition, gut microbiota also play an important role in the regulation of *Plasmodium* (malaria parasite) development. Thus, understanding the mechanism of microbial homeostasis in mosquito gut might be one of the strategies to manipulate malaria parasite development. In the present study, we characterized a 692 amino acids long secreted midgut heme-peroxidase 2 (AsHPX2) in *Anopheles stephensi*, the major Indian malaria vector. The presence of putative integrin binding motifs, LDV (Leu–Asp–Val), indicated its peroxinectin-like nature. Our phylogenetic analysis revealed that AsHPX2 is a Culicinae lineage-specific gene. RNA interference (RNAi)-mediated silencing of AsHPX2 gene significantly enhanced the growth of midgut bacteria in sugar-fed mosquitoes against sham-treated controls. Interestingly, blood-feeding drastically reduced AsHPX2 gene expression and enhanced the growth of midgut bacteria. These results revealed a negative correlation between the expression of AsHPX2 gene and gut bacterial growth. We proposed that AsHPX2, being a mosquito-specific gene, might serve as a "potent target" to manipulate midgut microbiota and vector competence.

Keywords: *Anopheles stephensi*, midgut, bacteria, heme-peroxidase, homeostasis, vector competence

INTRODUCTION

Newly emerged mosquitoes are born with a limited energy reserve and therefore, they start feeding the nectar to replenish energy in order to power the flight for swarming, mating and blood-seeking activities. The initial feeding behavior contributes to the establishment of the microbial community in the mosquito midgut. The midgut microbes facilitate food digestion, metabolism, detoxification and the development of immunity (Gusmão et al., 2007; Minard et al., 2013; Kajla et al., 2015).

Interestingly, the dynamic nature of gut microbiota is also associated with different stages of mosquito development as well as their nutritional conditions. For example, in sugar-fed mosquito

midguts cellulose degrading bacteria predominate, however, the bacteria facilitating blood digestion are more common in blood-fed midguts (de Gaio et al., 2011; Wang et al., 2011; Minard et al., 2013). In addition, the microbial interaction with mosquito midgut immunity also plays a pivotal role in the biological outcome of this symbiotic association. Thus, microbial homeostasis is managed by numerous immune mechanisms such as the production of lysozyme, reactive oxygen species (ROS), reactive nitrogen species (RNS), and antimicrobial peptides (AMPs) (Luckhart et al., 1998; Graca-Souza et al., 2006; Peterson and Luckhart, 2006; Brennan et al., 2008; Nishikori et al., 2009; Login et al., 2011; Wang et al., 2011).

It is also noteworthy to mention that the midgut microbiota also regulates *Plasmodium* development (Dong et al., 2009; Cirimotich et al., 2011). It was evident from numerous studies where co-feedings of either live or heat-killed bacteria decreased parasites number (Dong et al., 2009). Moreover, the parasite load also increased in antibiotics fed mosquitoes. Interestingly, the bacteria-induced ROS in mosquito midgut suppressed *Plasmodium* development (Beier et al., 1994; Dong et al., 2009; Cirimotich et al., 2011). Thus, we believe that the manipulation of midgut bacteria or mechanisms regulating bacterial homeostasis might be promising to alter the vectorial capacity (the property to support parasite development) of mosquito.

Heme-peroxidases regulate antibacterial pathways in mammals and insects. They catalyze H_2O_2-dependent oxidation of halides that, in turn, inhibit microbial metabolism and growth (Ha et al., 2005a; Klebanoff, 2005; Kumar et al., 2010; Kajla et al., 2016a). In addition, heme-peroxidases also catalyze the crosslinking of mucins layer over the midgut epithelium to block the interaction of lumen bacteria with mosquito immunity. This cross-linked barrier-based mechanism creates a low immunity zone in midgut to support the growth of microbial community (Kumar et al., 2010; Kajla et al., 2016a). Thus, mosquito peroxidases play a dramatic role in bacteria homeostasis and immunity.

Our analyses of *Anopheles stephensi* genome revealed the presence of 18 heme-peroxidases that participate in important biological functions (Kajla et al., 2016b; Choudhury et al., 2019; Kakani et al., 2019). In this study, we characterized *An. stephensi* midgut heme-peroxidase 2 (AsHPX2) and explored its role in the regulation of bacterial homeostasis. Our findings will open new opportunities to exploit the peroxidase-mediated immunemodulatory mechanism in mosquito for manipulating malaria parasite development.

MATERIALS AND METHODS

Ethics Statement
The use of experimental animals in this study was approved by the BITS, Pilani Institutional Animal Ethical Committee (Approval number IAEC/RES/18/02). Animal maintenance and experiments were performed in accordance with guidelines of the Committee for the Purpose of Control and Supervision of Experiments on Animals (CPCSEA), Government of India.

Rearing of Mosquitoes
Anopheles stephensi mosquitoes were reared in an insectary at Birla Institute of Technology and Science, Pilani, Rajasthan. The insectary was maintained at 28°C, 80% relative humidity (RH) and 12 h light:dark cycle as described before (Dhawan et al., 2017; Kajla et al., 2017). Adult mosquitoes were regularly fed on 10% sucrose solution. For colony propagation, 4- to 5-day-old females were fed on anesthetized mice and their eggs were collected in moist conditions. The hatched larvae were floated in water to continue the life cycle and fed on a 1:1 mixture of dog food (Pet Lover's crunch milk biscuit, India) and fish food (Gold Tokyo, India) (Gupta et al., 2017; Choudhury et al., 2019; Kakani et al., 2019).

Retrieval of Heme Peroxidase AsHPX2 Gene From *An. stephensi* Genome
Anopheles gambiae AgHPX2 gene (AGAP009033) was blast searched against the partially annotated genome of *An. stephensi* (taxid: 30069) to retrieve its ortholog. The best matching *An. stephensi* contig 7145 (SuperContig KB664566 and Ensembl identifier ASTE003848) was analyzed using Augustus software to identify the full-length putative AsHPX2 gene as before (Stanke et al., 2008; Choudhury et al., 2019; Kakani et al., 2019). AsHPX2 and AgHPX2 gene sequences were aligned to design gene-specific primers. The list of these primers is provided in **Supplementary Table S1**.

Cloning, Sequencing and Phylogenetic Analysis of AsHPX2
Full-length AsHPX2 gene was PCR amplified from *An. stephensi* midgut cDNA template using Phusion High-Fidelity DNA Polymerase (Thermo scientific, #F-530S) and F4R5 primers. PCR was initiated at 98°C for 30 s followed by 35 cycles at 98°C for 10 s, 62°C for 30 s and 72°C for 2 min. The final extension was carried at 72°C for 10 min. The amplified product was purified and sequenced at Eurofins genomics. The sequence identity of full-length AsHPX2 cDNA was confirmed through general BLAST and submitted to NCBI Genbank (accession numbers: KY363390).

The 5′ upstream region of AsHPX2 gene was analyzed by Augustus and JASPAR/MatInspector software to mark the putative promoter and regulatory sequences, respectively as before (Cartharius et al., 2005; Stanke et al., 2008; Mathelier et al., 2014; Kajla et al., 2016b; Kakani et al., 2019). The search criteria for these analyses were restricted to the transcription factors from insect family with minimum 80% similarity.

To analyze the evolutionary relationship of AsHPX2 protein, phylogenetic tree was constructed using the neighbor-joining (NJ) method implemented in MEGA 5.2 program as before (Saitou and Nei, 1987). The sequences of different animal heme peroxidases, implemented to construct the tree, were downloaded from NCBI and listed in **Supplementary Table S2**. The branching pattern reliability of the phylogenetic tree was tested by 1,000 bootstrap replicates.

In Silico Analysis of AsHPX2 Protein

Conserved domains in AsHPX2 protein were identified with the help of Conserved Domain Database (CDD) as well as SMART database (Letunic et al., 2014; Marchler-Bauer et al., 2015). The putative signal peptide in AsHPX2 protein was analyzed using SignalP and Phobius software (Käll et al., 2007; Petersen et al., 2011). The putative active sites and 3D structure of AsHPX2 protein was analyzed using Phyre^2 and TASSER software (Kelley et al., 2015; Yang et al., 2015). The quality of the predicted AsHPX2 model was assessed by TM-score (Zhang, 2008).

Collection of Different Mosquito Development Stages and Tissues

Different developmental stages of *An. stephensi* such as, eggs, first to fourth instar larvae, pupae, adult males or females were pooled and collected separately in RNAlater (Qiagen) and stored at −80°C. The midguts or carcasses (rest of the body parts after removing midguts) from sugar- or blood-fed females were also collected in a similar way. In some experiments, mosquitoes, as well as dissected midguts, were surface sterilized by rinsing them thrice, each for 5 s, in absolute ethanol and stored in RNAlater at −80°C (Gupta et al., 2009; Kumar et al., 2010; Wang et al., 2011).

RNA Isolation, cDNA Preparation and Analysis of Gene Expression

Total RNA was isolated from mosquito tissues by RNAeasy mini kit (Qiagen) and the first-strand cDNA was synthesized using Quantitect reverse transcription kit (Qiagen) that included a genomic wipeout treatment step to remove genomic DNA contamination. Since, the central gene of interest in this study is intronless, therefore, to insure no gDNA contamination in RNA preparations we included a negative RT control (i.e., a cDNA preparation using DNase-treated RNA and all reaction components except the RT enzyme) in the qPCR analyses. The IQ5 multicolor real-time PCR detection system (Bio-Rad) was used to analyze the relative mRNA expressions of AsHPX2 gene and the bacterial load was determined by the amplification of 16S rRNA gene. The sequences of all the mosquito gene primers and universal 16S primers are listed in **Supplementary Table S1**. The ribosomal protein subunit S7 mRNA was used as an internal loading control as before (Kumar et al., 2010; Dixit et al., 2011; Kakani et al., 2019). PCR cycle parameters were following: 95°C for 5 min, 40 cycles each at 94°C for 20 s, 55°C for 30 s, and 72°C for 50 s. Fluorescence was read at 72°C after each cycle. The final extension was carried at 72°C for 10 min and then subjected to a melting curve to confirm the identity of PCR product. The end product was run on a gel to confirm the specificity of primers. Relative mRNA levels of various genes were calculated using $^{\Delta\Delta}$Ct method as before (Livak and Schmittgen, 2001; Kumar et al., 2010; Kakani et al., 2019). The PCR amplification efficiency was determined with LinRegPCR as described elsewhere (Ramakers et al., 2003).

dsRNA Synthesis and Gene Silencing

A 450-bp fragment of AsHPX2 cDNA was amplified using F1R1 primers (**Supplementary Table S1**) and cloned into the pCRII-TOPO vector. Similarly, a 218-bp fragment of LacZ gene was amplified and cloned using the primers (5′ to 3′) F-GAGTCAGTGAGCGAGGAAGC and R-TATCCGCTCACAATTCCACA (Gupta et al., 2009; Kajla et al., 2017). These clones already have a T7 promoter site at one end thus, another T7 promoter was incorporated at the other end of the fragment by amplifying the insert with the primers: M13F-GTAAAACGACGGCCAGT and T7-M13R-CTCGAGTAATACGACTCACTATAGGGCAGGAAACAGCTATGAC. PCR cycle parameters were following: 94°C for 5 min followed by 40 cycles each with 94°C for 30 s, 55°C for 30 s, and 72°C for 30 s. The final extension was carried at 72°C for 10 min. Amplicons were extracted from the gel with QIAquick Gel Extraction Kit (Qiagen) and used to synthesize dsRNA as per the instructions of MEGAscript RNAi kit (Ambion). dsRNA was purified with the help of Microcon YM-100 filter (Millipore) and finally concentrated to 3 µg/µl in DNase- and RNase-free water (Dhawan et al., 2017; Kajla et al., 2017; Kakani et al., 2019).

For gene silencing, 2-day-old female mosquitoes were injected with 69 nl of 3 µg/µl dsAsHPX2 (silenced) or dsLacZ (control) RNA into their thorax using a nanojector (Drummond). Four days after the injection, mosquitos were surface sterilized and their midguts were dissected as before (Gupta et al., 2009; Kumar et al., 2010; Wang et al., 2011).

Statistical Analysis of the Data

All the data were expressed as a mean ± standard deviation. GraphPad Prism 5.0 software was used to analyze statistical significance between test and respective controls by performing Student's *t*-test or one-way ANOVA (Motulsky, 1999). The data were considered significant if $p < 0.05$. Each experiment was performed at least thrice to validate the findings.

RESULTS

Cloning and Characterization of AsHPX2 Gene

Putative AsHPX2 gene was identified in contig 7,145 of un-annotated *An. stephensi* genome as described in the Materials and Methods. Analysis of this contig by Augustus software predicted 2,868 bp full-length AsHPX2 gene containing 2,079 bp open reading frame (ORF), which encodes for a 692 amino acids long protein. The 5′-untranslated region (5′-UTR) and 3′-UTR of AsHPX2 gene were found to be 438 and 351 bp, respectively. The polyadenylation signal AATAAA was identified 331 bp downstream from the stop codon (**Supplementary Figure S1**).

Furthermore, the 5′ upstream region of AsHPX2 gene was analyzed by JASPAR and MatInspector software to identify putative transcription factor binding motifs (TFBM) in its promoter region. Our analyses indicated the binding sites for some major transcription factors such as, GATA (pnr), Rel1, AP-1 (a Jun/Fos dimer) and Broad complex (Br-C) (**Supplementary Figure S1**) that indicated a tissue-specific immune role of AsHPX2 in a way similar to other insect genes (Senger et al., 2006; Zhu et al., 2007; Garver et al., 2013; Kajla et al., 2016b; Zakovic and Levashina, 2017; Kakani et al., 2019).

The predicted AsHPX2 cDNA sequence was aligned with *An. gambiae* AgHPX2 (AGAP009033) gene to design gene-specific primers (**Supplementary Table S1**) and F4R5 primers set amplified ∼2 kb full-length gene from *An. stephensi* cDNA (**Figure 1**). The PCR product was sequenced and blast search revealed its 80% identity with AgHPX2 gene (*e* value $3e^{-107}$). This sequence was submitted to NCBI (GenBank accession number: KY363390) and its alignment with the predicted *An. stephensi* genomic DNA revealed that AsHPX2 is an intron-less gene (**Figure 1**) in a way similar to its ortholog AgHPX2 (Giraldo-Calderón et al., 2015).
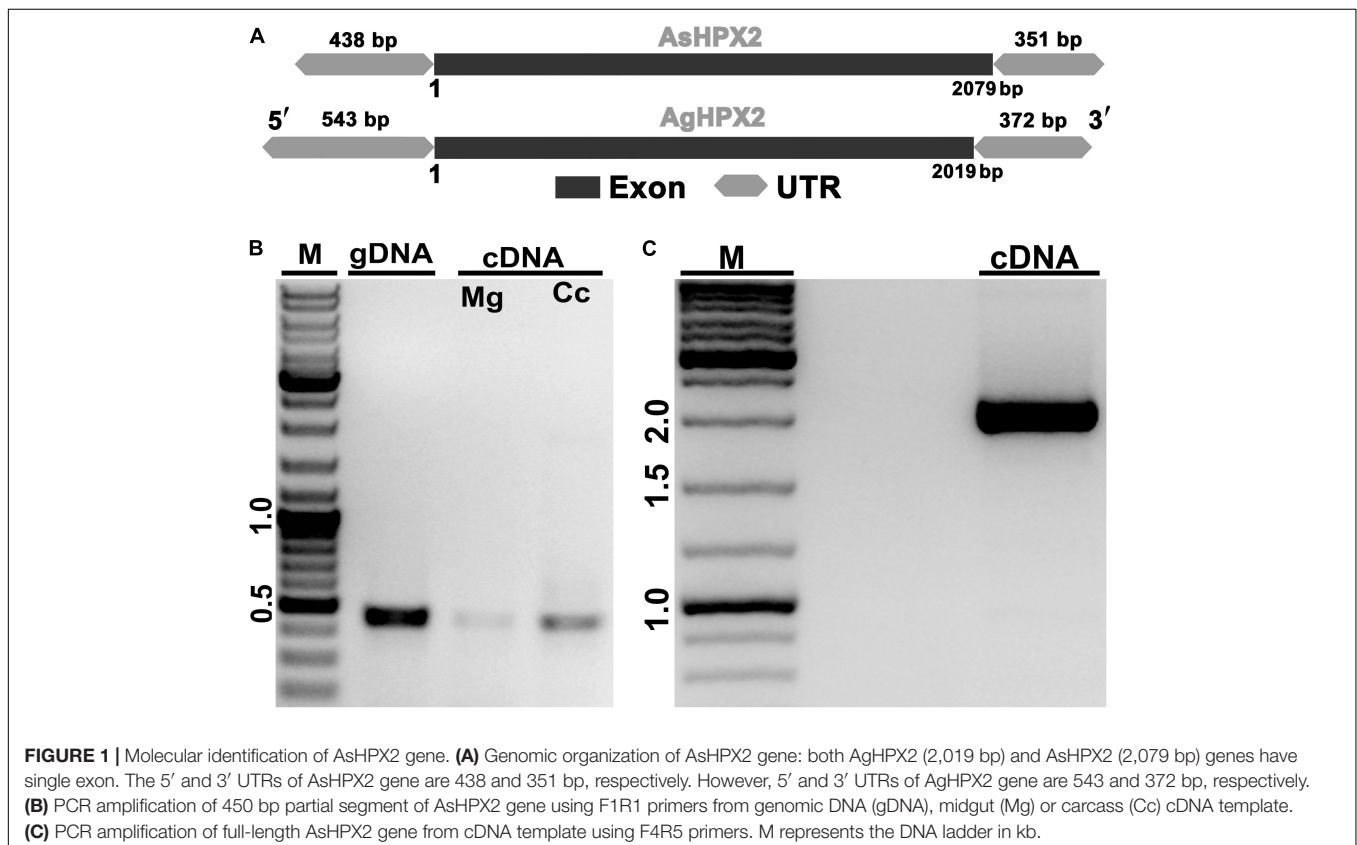
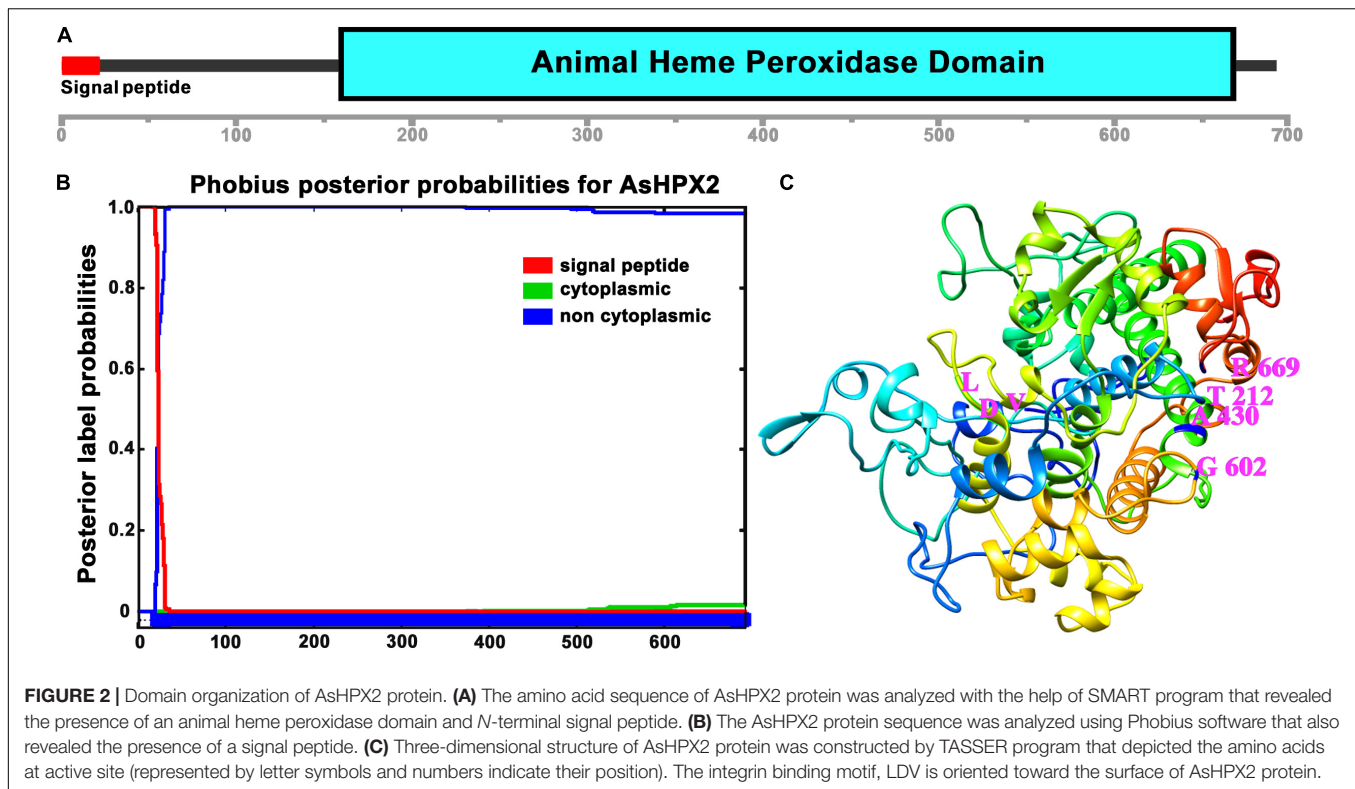## Sequence and Domain Analysis of AsHPX2 Protein

Analyses of 76.9 kDa AsHPX2 protein by SMART program revealed that it is an animal heme-peroxidase (**Figure 2**). The presence of a 21 amino acids long signal peptide and signal peptidase cleavage site between Gly_{21} and Arg_{22} residues at *N*-terminal suggested that AsHPX2 is a secreted protein (**Figure 2B**). Phyre^2 software analyses revealed the presence of 47% alpha helices in the secondary structure of AsHPX2 protein (**Supplementary Figure S2**) indicating that it is a globular protein as suggested by others (Pace and Scholtz, 1998; Kajla et al., 2016b). In addition, this protein also contains 10 heme-binding sites, 13 substrate-binding sites, three calcium-binding sites, and three homodimer interface sites (**Supplementary Figure S2**) in a way similar to other insect heme-peroxidases (Soudi et al., 2012;

Kajla et al., 2016b; Bailey et al., 2017; Choudhury et al., 2019; Kakani et al., 2019). Three-dimensional structure of AsHPX2 protein (TM-score 0.70 ± 0.12) revealed the presence of catalytic quartet (Thr_{212}, Ala_{430}, Gly_{602}, and Arg_{669}), which is positioned toward the protein surface. Interestingly, the presence of a surface oriented triplet of Leu_{530}, Asp_{531}, and Val_{532} (LDV), which constitutes an integrin binding motif, indicated that AsHPX2 is a peroxinectin-like protein (**Figures 2B,C**) and might participate in cell adhesion as suggested by others (Johansson et al., 1995; Ruoslahti, 1996; Johanssen et al., 1999).

Sequence Homology and Phylogenetic Analysis of AsHPX2 Protein

The sequence of AsHPX2 protein was aligned with heme-peroxidases from other organisms as listed in **Supplementary Table S2** to analyze their sequence conservation. AsHPX2 shared 79 and 73% identity with *An. gambiae* AgHPX2 and *An. sinensis* AsnHPX2, respectively (**Supplementary Table S2**). On the other hand, it shared 57, 59, and 58% identity with *Aedes aegypti* AeHPX2, *Ae. albopictus* AaHPX2, and *Culex quinquefasciatus* CqHPX2, respectively. Interestingly, AsHPX2 protein shared only 34% identity with *Drosophila melanogaster* immune-related catalase (IRC), a heme-peroxidase that performs catalase cycle (Ha et al., 2005a,b). In addition, it shared less than 30% identity with human peroxidases (**Supplementary Table S2**). Evolutionary relationship of AsHPX2 protein with heme-peroxidases from other organisms

FIGURE 1 | Molecular identification of AsHPX2 gene. **(A)** Genomic organization of AsHPX2 gene: both AgHPX2 (2,019 bp) and AsHPX2 (2,079 bp) genes have single exon. The 5′ and 3′ UTRs of AsHPX2 gene are 438 and 351 bp, respectively. However, 5′ and 3′ UTRs of AgHPX2 gene are 543 and 372 bp, respectively. **(B)** PCR amplification of 450 bp partial segment of AsHPX2 gene using F1R1 primers from genomic DNA (gDNA), midgut (Mg) or carcass (Cc) cDNA template. **(C)** PCR amplification of full-length AsHPX2 gene from cDNA template using F4R5 primers. M represents the DNA ladder in kb.

FIGURE 2 | Domain organization of AsHPX2 protein. **(A)** The amino acid sequence of AsHPX2 protein was analyzed with the help of SMART program that revealed the presence of an animal heme peroxidase domain and *N*-terminal signal peptide. **(B)** The AsHPX2 protein sequence was analyzed using Phobius software that also revealed the presence of a signal peptide. **(C)** Three-dimensional structure of AsHPX2 protein was constructed by TASSER program that depicted the amino acids at active site (represented by letter symbols and numbers indicate their position). The integrin binding motif, LDV is oriented toward the surface of AsHPX2 protein.

(as mentioned in **Supplementary Table S2**) also revealed that mosquito HPX2s appeared in a single cluster and are diverged from *D. melanogaster* IRC (**Supplementary Figure S3**). Human peroxidases appeared in a separate cluster far away from mosquito HPX2 peroxidases.

AsHPX2 Is Distinctively Expressed in Different Developmental Stages of Mosquito

The expression of AsHPX2 gene in different developmental stages of *An. stephensi* was analyzed by qRT-PCR. AsHPX2 gene is expressed throughout all developmental stages of *An. stephensi* namely, eggs, first to fourth instar larvae, pupae, adult males or females (**Figure 3**). The relative mRNA levels of AsHPX2 gene were 6-fold, 4-fold, 2.5-fold, and 0.65-fold in first, second, third, and fourth instar larvae, respectively when compared to the eggs ($p = 0.0087$, $p = 0.0024$, $p = 0.0030$, and $p = 0.0148$, respectively). Furthermore, the relative AsHPX2 mRNA levels were 2-fold, 26-fold and 84-fold in pupae, adult males and females, respectively, against eggs ($p = 0.0012$, $p = 0.0008$, and $p = 0.0005$, respectively) (**Figure 3**).

Blood-Feeding Down Regulates the Expression of AsHPX2 Gene
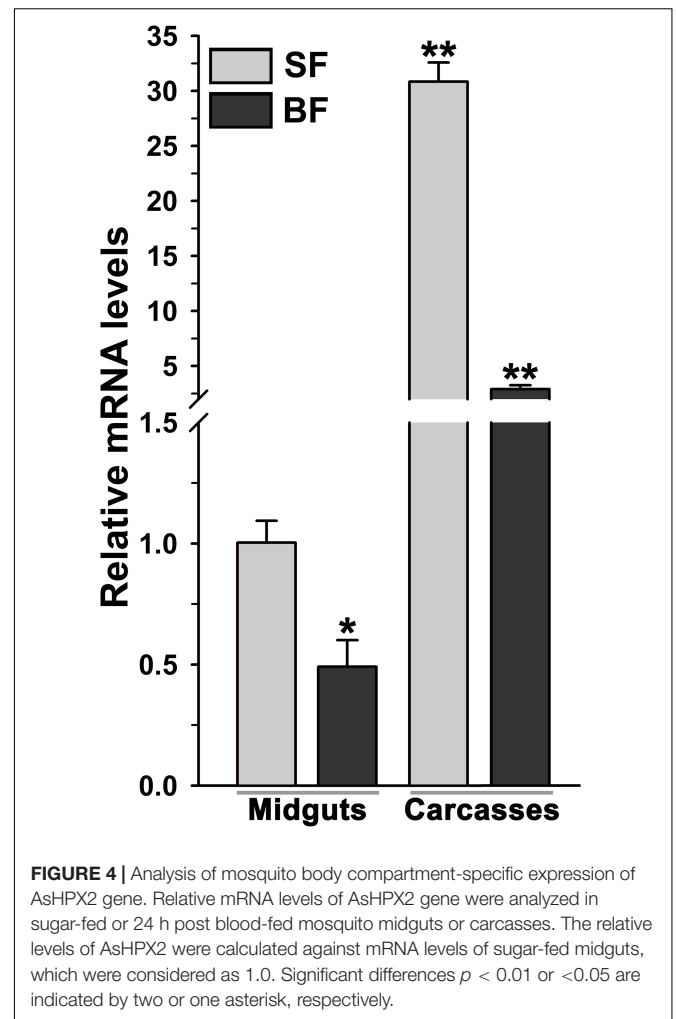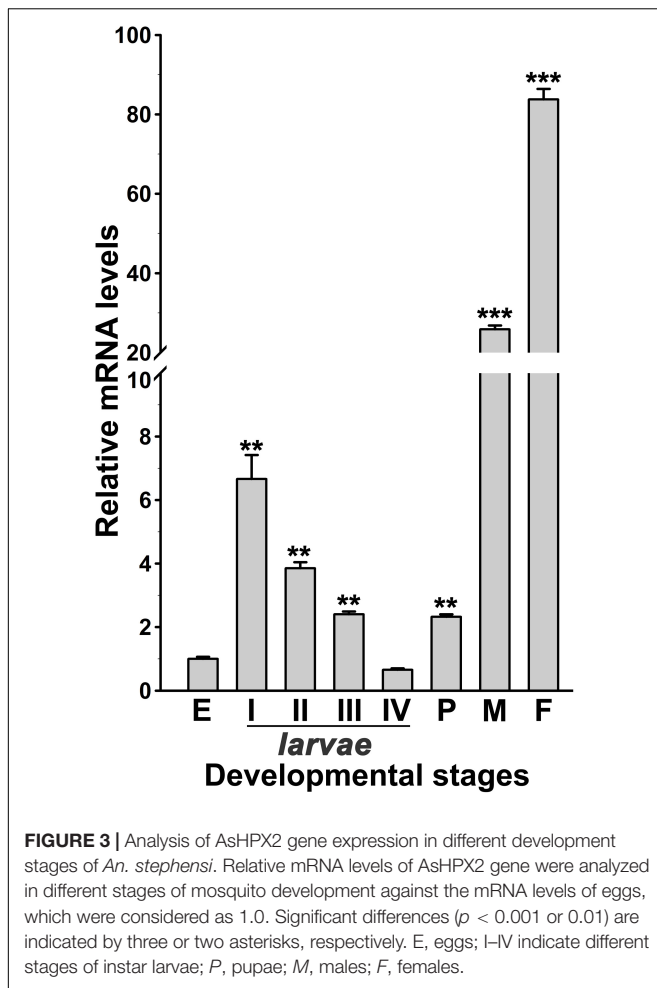
The relative mRNA levels of AsHPX2 gene were analyzed in sugar- or 24 h post blood-fed midguts or carcasses to decipher its tissue-specific expression. The results presented in **Figure 4**

showed that AsHPX2 mRNA levels were 33-fold higher in sugar-fed carcasses than midguts ($p = 0.0017$). Moreover, its mRNA levels were reduced twofold ($p = 0.0367$) and 10-fold ($p = 0.0020$) in 24 h post blood-fed midguts and carcasses, respectively against their sugar-fed controls. In addition, the time kinetics also revealed that the midgut expression of AsHPX2 gene is down regulated after blood-feeding when compared to the sugar-fed controls (**Figure 5**).

The downregulation of AsHPX2 gene expression in blood-fed midguts might be explained by the presence of Z3 isoform of Br-C TFBM in its regulatory region (**Supplementary Figure S1**), which restricts tissue- and condition-specific expression of the gene (Von Kalm et al., 1994; Bayer et al., 1996; Chen et al., 2004; Zhu et al., 2007).

AsHPX2 Regulates the Bacterial Homeostasis in Midgut

The domain analyses revealed that AsHPX2 exhibits peroxinectin-like nature (has cell adhesive property and role in immunity) (**Figure 2C** and **Supplementary Figure S2**). Thus, we hypothesized that AsHPX2 gene might regulating bacterial homeostasis in mosquito midguts. To demonstrate this, AsHPX2 gene was silenced in the midguts of sugar-fed mosquitoes as described in Materials and Methods and its effect was evaluated on the levels of endogenous bacteria. Our analyses of AsHPX2 mRNA levels in controls and silenced midguts revealed 90% silencing of this gene ($p = 0.0006$, **Figure 6**). Furthermore, the analyses of 16S rRNA levels of endogenous bacteria in these samples indicated that their levels increased ∼4-fold in silenced

FIGURE 3 | Analysis of AsHPX2 gene expression in different development stages of *An. stephensi*. Relative mRNA levels of AsHPX2 gene were analyzed in different stages of mosquito development against the mRNA levels of eggs, which were considered as 1.0. Significant differences ($p < 0.001$ or 0.01) are indicated by three or two asterisks, respectively. E, eggs; I–IV indicate different stages of instar larvae; P, pupae; M, males; F, females.

FIGURE 4 | Analysis of mosquito body compartment-specific expression of AsHPX2 gene. Relative mRNA levels of AsHPX2 gene were analyzed in sugar-fed or 24 h post blood-fed mosquito midguts or carcasses. The relative levels of AsHPX2 were calculated against mRNA levels of sugar-fed midguts, which were considered as 1.0. Significant differences $p < 0.01$ or <0.05 are indicated by two or one asterisk, respectively.

midguts against controls ($p = 0.0012$, **Figure 6**). These results established the antibacterial role of AsHPX2 gene.
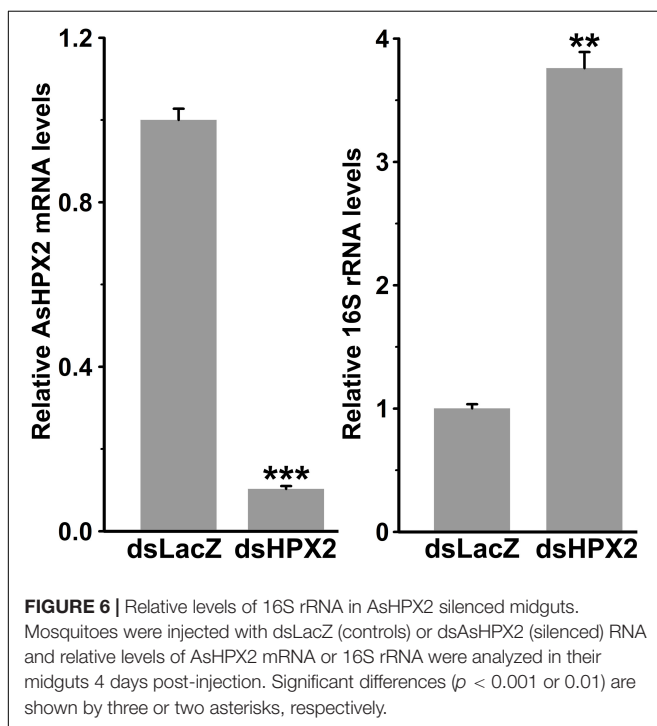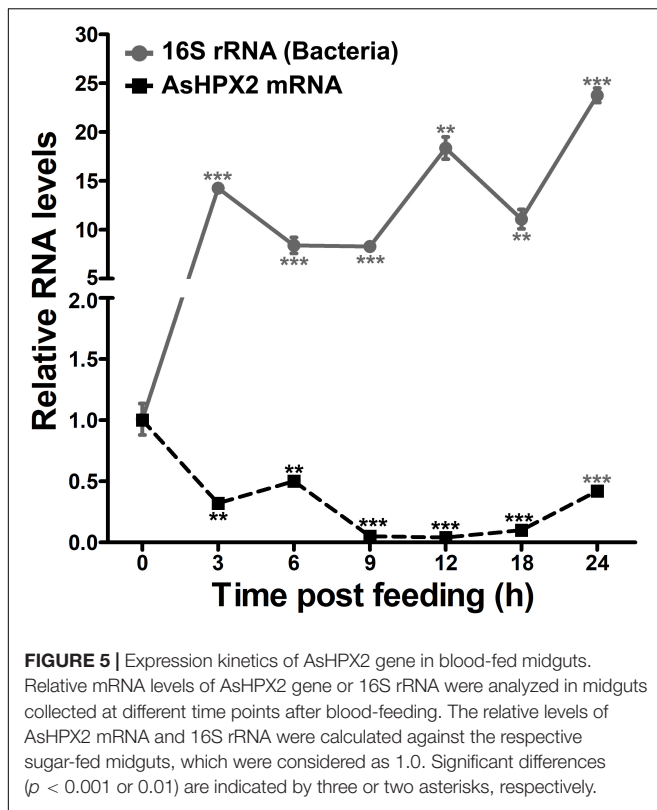
The silencing of AsHPX2 gene increased bacterial load in the midguts of sugar fed mosquitoes (**Figure 6**). Interestingly, our time kinetics study revealed that blood-feeding induced the growth of midgut bacteria (**Figure 5**) in a similar way as reported in our previous publications as well as by others (Kumar et al., 2010; Oliveira et al., 2011; Habtewold et al., 2016; Kajla et al., 2016a). However, on the other hand, there is an inverse correlation between the increased growth of bacteria and expression of AsHPX2 gene in blood-fed midguts (**Figure 5**). Thus, we believe that the down regulation of AsHPX2 gene in blood fed midguts (**Figures 4**, **5**) augments the growth of midgut bacteria to support blood digestion.

Together, we proposed a putative model that describes the role of AsHPX2 gene in maintaining gut microbiome homeostasis as depicted in **Figure 7**. In brief, AsHPX2, a peroxinectin-like peroxidase limits the growth of bacteria in sugar-fed midguts most probable through the formation of hypochlorous acid (HOCl) produced from H_2O_2 and halides via halogenation cycle (Klebanoff, 1968; Klebanoff, 2005; Allen and Stephens, 2011). After a blood meal, AsHPX2 gene down-regulation (**Figure 5**)

and up-regulation of another heme-peroxidase AsHPX15 that catalyzes the crosslinking of mucins barrier over the immune reactive midgut epithelium (Kumar et al., 2010; Kajla et al., 2015, 2016b) collectively promote the growth of endogenous bacteria to support various life processes such as digestion and reproduction (Oliveira et al., 2011; Kajla et al., 2015; Habtewold et al., 2016).

DISCUSSION

In this study, we characterized AsHPX2 gene from *An. stephensi* mosquito that encodes for a 692 amino acid long secreted protein. Interestingly, the intronless nature of AsHPX2 gene indicates that it has a tissue-specific expression with a high rate of evolution in a way similar to other intronless genes such as calmodulin-like gene NB1 and Poly(A) polymerase in human (Le et al., 2001; Shabalina et al., 2010). AsHPX2 has >70 and $<60\%$ amino acid identity with anopheline and Culicinae HPX2s, respectively. However, it shares $<35\%$ identity with human peroxidases and *D. melanogaster* IRC, a heme-peroxidase that performs catalase cycle (Ha et al., 2005a,b). In conclusion,
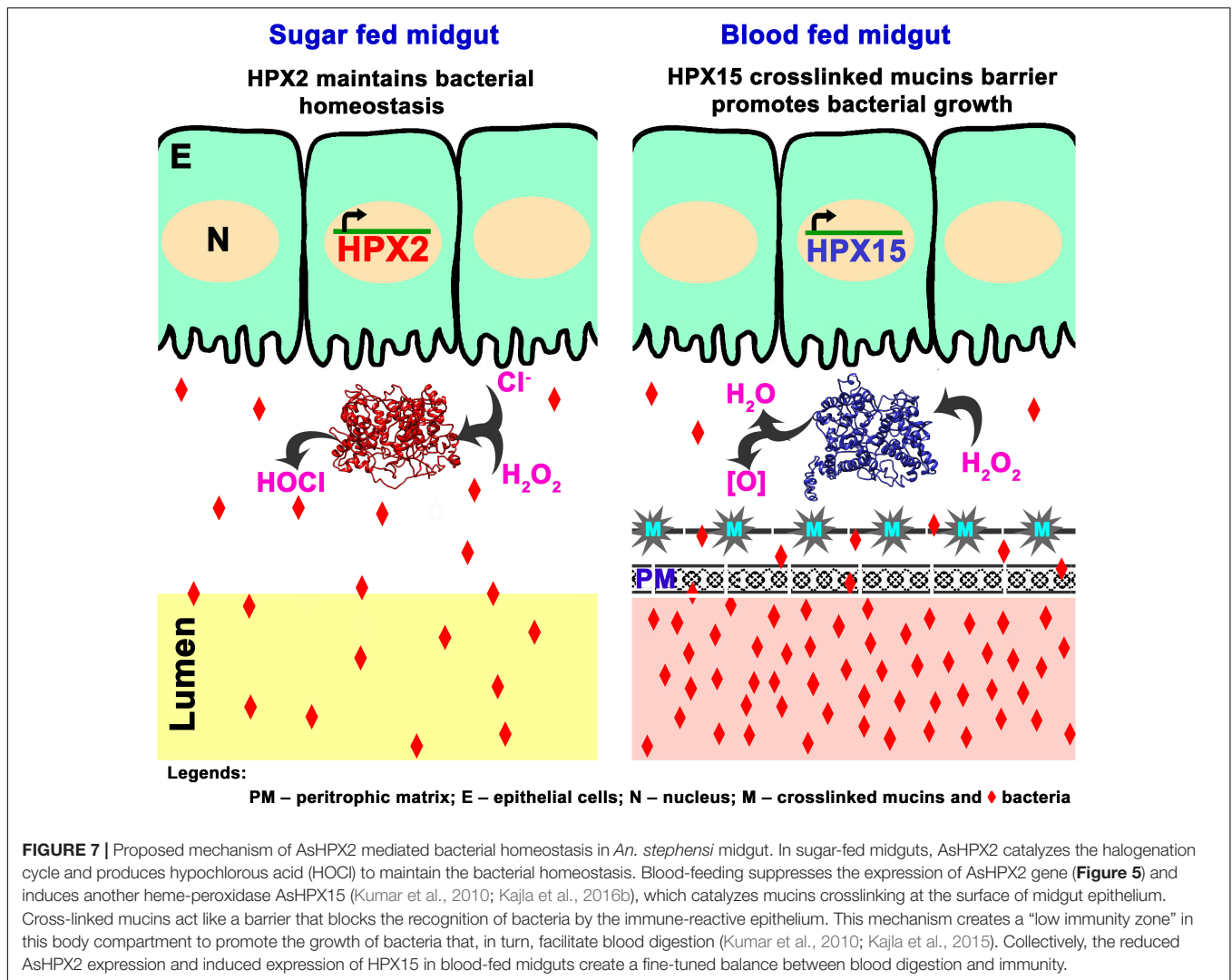
FIGURE 5 | Expression kinetics of AsHPX2 gene in blood-fed midguts. Relative mRNA levels of AsHPX2 gene or 16S rRNA were analyzed in midguts collected at different time points after blood-feeding. The relative levels of AsHPX2 mRNA and 16S rRNA were calculated against the respective sugar-fed midguts, which were considered as 1.0. Significant differences ($p < 0.001$ or 0.01) are indicated by three or two asterisks, respectively.

FIGURE 6 | Relative levels of 16S rRNA in AsHPX2 silenced midguts. Mosquitoes were injected with dsLacZ (controls) or dsAsHPX2 (silenced) RNA and relative levels of AsHPX2 mRNA or 16S rRNA were analyzed in their midguts 4 days post-injection. Significant differences ($p < 0.001$ or 0.01) are shown by three or two asterisks, respectively.

these data indicated that AsHPX2 is a mosquito-specific gene. The presence of different TFBM in the regulatory region of AsHPX2 gene signifies its importance in mosquito biology. For

example, GATA (pnr) and Br-C binding might explain its tissue-specific expression and down-regulation in blood-fed midguts, respectively in a way similar to other insect genes (Von Kalm et al., 1994; Bayer et al., 1996; Chen et al., 2004; Senger et al., 2006; Zhu et al., 2007; Kajla et al., 2016b; Kakani et al., 2019). It is noteworthy to mention that Br-C isoforms are activated in response to the blood-feeding induced ecdysone. Interestingly, out of four different isoforms of Br-C (Z1 to Z4), any one of them can circumstantially either induce or suppress a target gene (Von Kalm et al., 1994; Edgar, 2006; Zhu et al., 2007). For example, a robust expression of vitellogen gene is induced by Z2 isoform of Br-C in mosquito fat body within 24 h of blood-feeding. However, Z1 and Z4 isoforms of Br-C ensure the termination of vitellogen gene expression after 24 h post blood meal (Zhu et al., 2007). In summary, Br-C isoforms participate in the regulation of specific gene(s) in a coordinated and well-orchestrated way.

The presence of integrin binding motif (LDV) in AsHPX2 protein suggested its peroxinectin-like nature. Peroxinectins are invertebrate peroxidases that are involved in cell adhesion (Liu et al., 2004; Vizzini et al., 2013; Shanthi et al., 2014). Interestingly, the surface orientation of LDV motif in AsHPX2 protein seems to be facilitating its adhesion in a way similar to other adhesion molecules (Johanssen et al., 1999; Liu et al., 2005). Peroxinectins selectively bind to the bacteria and catalyze the formation of HOCl, an anti-bacterial molecule, through halogenation cycle (Klebanoff, 1968, 2005; Allen and Stephens, 2011). Interestingly, peroxinectins also bind superoxide dismutase (SOD), an enzyme that catalyzes the formation of H_2O_2 from superoxide anions, which, in turn, promotes the continuity of halogenation cycle (Holmblad and Soderhall, 1999; Johanssen et al., 1999; Choudhury et al., 2019).

Differential expression of AsHPX2 gene in different stages of mosquito development corroborates with the expression profile of some peroxidases (Mdes000915, Mdes001004, Mdes009520, and Mdes015930) across the developmental stages of Hessian fly *Mayetiola destructor* (Chen et al., 2016). Because peroxidases catalyze the crosslinking of biological matrices and regulate immune functions thus, their expression might reveal a direct association to the immune status and/or bacterial homeostasis during insect development. Direct evidence for this belief was reported in *An. gambiae* where a dynamic mosquito gut microbiome is associated with transitions in developmental stages and alteration of feeding behavior from the sugar diet to blood meal (Wang et al., 2011).

AsHPX2 gene silencing significantly enhanced the growth of midgut bacteria that revealed its antibacterial role in sugar fed mosquitoes. Therefore, the downregulation of AsHPX2 gene expression in blood-fed midguts is an important event and it is inversely correlated to the growth of bacteria. Because the bacteria play an important role in blood digestion thus, down-regulation of AsHPX2 gene creates a physiological condition in blood-fed midguts to facilitate digestion (Kumar et al., 2010; de Gaio et al., 2011; Kajla et al., 2015). Our results indicated that AsHPX2 is one of the important regulators that maintain homeostasis of endogenous bacteria in sugar- or

FIGURE 7 | Proposed mechanism of AsHPX2 mediated bacterial homeostasis in *An. stephensi* midgut. In sugar-fed midguts, AsHPX2 catalyzes the halogenation cycle and produces hypochlorous acid (HOCl) to maintain the bacterial homeostasis. Blood-feeding suppresses the expression of AsHPX2 gene (**Figure 5**) and induces another heme-peroxidase AsHPX15 (Kumar et al., 2010; Kajla et al., 2016b), which catalyzes mucins crosslinking at the surface of midgut epithelium. Cross-linked mucins act like a barrier that blocks the recognition of bacteria by the immune-reactive epithelium. This mechanism creates a "low immunity zone" in this body compartment to promote the growth of bacteria that, in turn, facilitate blood digestion (Kumar et al., 2010; Kajla et al., 2015). Collectively, the reduced AsHPX2 expression and induced expression of HPX15 in blood-fed midguts create a fine-tuned balance between blood digestion and immunity.

blood-fed midguts. Interestingly, blood-feeding up-regulates the expression of another heme-peroxidase, AsHPX15 that catalyzes the crosslinking of mucins barrier over the immune reactive midgut epithelium to protect the growing bacteria (Kumar et al., 2010; Kajla et al., 2015, 2016b).

Thus, the systematic regulation of bacterial antagonistic (AsHPX2) and agonistic (AsHPX15) peroxidases create a low immunity zone in midgut for promoting the growth of bacteria, facilitating blood digestion and maintaining a fine balance between food digestion and immunity. Hence, the regulated expression of heme-peroxidases is one of the mechanisms that actively maintain bacterial homeostasis in mosquito midgut during distinctive nutritional conditions.

In conclusion, the identification of *Anopheles* genes that maintain microbial homeostasis in the midgut are of great value as they can be exploited to achieve dysbiosis of the mosquito gut ecosystem and hence, the vector competence. Overall, from the present study, it is clear that AsHPX2 is a mosquito-specific gene that plays an important role in

midgut physiology and immunity. Hence, this gene can be a potent target to alter the bacterial community and regulating *Plasmodium* development.

DATA AVAILABILITY STATEMENT

The raw data supporting the conclusions of this article will be made available by the authors, without undue reservation.

ETHICS STATEMENT

The animal study was reviewed and approved by BITS, Pilani Institutional Animal Ethical Committee.

AUTHOR CONTRIBUTIONS

PK, LG, and SK designed the experiments, performed expression kinetics of AsHPX2 and silencing experiments, analyzed the

data, and wrote the manuscript. PK and SK collected samples to perform experiments. All authors approved the manuscript.

FUNDING

ACKNOWLEDGMENTS

SUPPLEMENTARY MATERIAL

The Supplementary Material for this article can be found online at: https://www.frontiersin.org/articles/10.3389/fphys.2020.572340/full#supplementary-material

REFERENCES

Allen, R. C., and Stephens, J. T. Jr. (2011). Myeloperoxidase selectively binds and selectively kills microbes. *Infect. Immun.* 79, 474–485. doi: 10.1128/iai.00910-09

Bailey, D., Basar, M. A., Nag, S., Bondhu, N., Teng, S., and Duttaroy, A. (2017). The essential requirement of an animal heme peroxidase protein during the wing maturation process in Drosophila. *BMC Dev. Biol.* 17:1. doi: 10.1186/s12861-016-0143-8

Bayer, C. A., Holley, B., and Fristrom, J. W. (1996). A switch in broad-complex zinc-finger isoform expression is regulated posttranscriptionally during the metamorphosis of *Drosophila* imaginal discs. *Dev. Biol.* 177, 1–14. doi: 10.1006/dbio.1996.0140

Beier, M. S., Pumpuni, C. B., Beier, J. C., and Davis, J. R. (1994). Effects of para-aminobenzoic acid, insulin, and gentamycin on *Plasmodium falciparum* development in Anopheline mosquitoes (Diptera: Culicidae). *J. Med. Entomol.* 31, 561–565. doi: 10.1093/jmedent/31.4.561

Brennan, L. J., Keddie, B. A., Braig, H. R., and Harris, H. L. (2008). The endosymbiont *Wolbachia pipientis* induces the expression of host antioxidant. *PLoS One* 3:e2083. doi: 10.1371/journal.pone.0002083

Cartharius, K., Frech, K., Grote, K., Klocke, B., Haltmeier, M., Klingenhoff, A., et al. (2005). MatInspector and beyond: promoter analysis based on transcription factor binding sites. *Bioinformatics* 21, 2933–2942. doi: 10.1093/bioinformatics/bti473

Chen, L., Zhu, J., Sun, G., and Raikhel, A. S. (2004). The early gene broad is involved in the ecdysteroid hierarchy governing vitellogenesis of the mosquito *Aedes aegypti*. *J. Mol. Endocrinol.* 33, 743–761. doi: 10.1677/jme.1.01531

Chen, M.-S., Liu, S., Wang, H., Cheng, X., El Bouhssini, M., and Whitworth, R. J. (2016). Massive shift in gene expression during transitions between developmental stages of the gall midge, *Mayetiola Destructor*. *PLoS One* 11:e0155616. doi: 10.1371/journal.pone.0155616

Choudhury, T. P., Gupta, L., and Kumar, S. (2019). Identification, characterization and expression analysis of *Anopheles stephensi* double peroxidase. *Acta Trop.* 190, 210–219. doi: 10.1016/j.actatropica.2018.10.008

Cirimotich, C. M., Dong, Y., Clayton, A. M., Sandiford, S. L., Souza-Neto, J. A., Mulenga, M., et al. (2011). Natural microbe-mediated refractoriness to *Plasmodium* infection in *Anopheles gambiae*. *Science* 332, 855–858. doi: 10.1126/science.1201618

de Gaio, A., Gusmão, D. S., Santos, A. V., Berbert-Molina, M. A., Pimenta, P. F., and Lemos, F. J. (2011). Contribution of midgut bacteria to blood digestion and egg production in *Aedes aegypti* (diptera: culicidae) (L.). *Parasit Vect.* 4:105. doi: 10.1186/1756-3305-4-105

Dhawan, R., Gupta, K., Kajla, M., Kakani, P., Choudhury, T. P., Kumar, S., et al. (2017). Apolipophorin-III acts as a positive regulator of *plasmodium* development in *Anopheles stephensi*. *Front. Physiol.* 8:185. doi: 10.3389/fphys.2017.00185

Dixit, R., Rawat, M., Kumar, S., Pandey, K. C., Adak, T., and Sharma, A. (2011). Salivary gland transcriptome analysis in response to sugar feeding in malaria

vector *Anopheles stephensi*. *J. Insect Physiol.* 57, 1399–1406. doi: 10.1016/j.jinsphys.2011.07.007

Dong, Y., Manfredini, F., and Dimopoulos, G. (2009). Implication of the mosquito midgut microbiota in the defense against malaria parasites. *PLoS Pathog.* 5:e1000423. doi: 10.1371/journal.ppat.1000423

Edgar, B. A. (2006). How flies get their size: genetics meets physiology. *Nat. Rev. Genet.* 7, 907–916. doi: 10.1038/nrg1989

Garver, L. S., de Almeida Oliveira, G., and Barillas-Mury, C. (2013). The JNK pathway is a key mediator of *Anopheles gambiae* antiplasmodial immunity. *PLoS Pathog.* 9:e1003622. doi: 10.1371/journal.ppat.1003622

Giraldo-Calderón, G. I., Emrich, S. J., MacCallum, R. M., Maslen, G., Dialynas, E., Topalis, P., et al. (2015). . VectorBase: an updated bioinformatics resource for invertebrate vectors and other organisms related with human diseases. *Nucl. Acids Res.* 43, D707–D713. doi: 10.1093/nar/gku1117

Graca-Souza, A. V., Maya-Monteiro, C., Paiva-Silva, G. O., Braz, G. R., and Paes, M. C. (2006). Adaptations against heme toxicity in blood-feeding arthropods. *Insect Biochem. Mol. Biol.* 36, 322–335. doi: 10.1016/j.ibmb.2006.01.009

Gupta, K., Dhawan, R., Kajla, M., Misra, T., Kumar, S., and Gupta, L. (2017). The evolutionary divergence of STAT transcription factor in different *Anopheles* species. *Gene* 596, 89–97. doi: 10.1016/j.gene.2016.09.022

Gupta, L., Molina-Cruz, A., Kumar, S., Rodrigues, J., Dixit, R., Zamora, R. E., et al. (2009). The STAT pathway mediates late-phase immunity against *Plasmodium* in the mosquito *Anopheles gambiae*. *Cell Host Microbe* 5, 498–507. doi: 10.1016/j.chom.2009.04.003

Gusmão, D. S., Santos, A. V., Marini, D. C., Russo, Ede, S., Peixoto, A. M., et al. (2007). First isolation of microorganisms from the gut diverticulum of *Aedes aegypti* (Diptera: Culicidae): new perspectives for an insect-bacteria association. *Mem. Inst. Oswaldo Cruz* 102, 919–924. doi: 10.1590/s0074-02762007000800005

Ha, E. M., Oh, C. T., Bae, Y. S., and Lee, W. J. (2005a). A direct role for dual oxidase in *Drosophila* gut immunity. *Science* 310, 847–850. doi: 10.1126/science.1117311

Ha, E. M., Oh, C. T., Ryu, J. H., Bae, Y. S., Kang, S. W., Jang, I. H., et al. (2005b). An antioxidant system required for host protection against gut infection in *Drosophila*. *Dev. Cell.* 8, 125–132. doi: 10.1016/j.devcel.2004.11.007

Habtewold, T., Duchateau, L., and Christophides, G. K. (2016). Flow cytometry analysis of the microbiota associated with the midguts of vector mosquitoes. *Parasit Vect.* 9:167. doi: 10.1186/s13071-016-1438-0

Holmblad, T., and Soderhall, K. (1999). Cell adhesion molecules and antioxidative enzymes in a crustacean, possible role in immunity. *Aquaculture* 172, 111–123. doi: 10.1016/s0044-8486(98)00446-3

Johanssen, M. W., Holmblad, T., ThoÈrnqvist, P.-O., Cammarata, M., Parrinello, N., and SoÈderhall, K. (1999). A cell-surface superoxide dismutase is a binding protein for peroxinectin, a cell-adhesive peroxidase in crayfish. *J. Cell. Sci.* 112, 917–925.

Johansson, M. W., Lind, M. I., Holmblad, T., Thörnqvist, P. O., and Söderhäll, K. (1995). Peroxinectin, a novel cell adhesion protein from crayfish, blood. *Biochem. Biophys. Res. Commun.* 216, 1079-1087.

Kajla, M., Choudhury, T. P., Kakani, P., Gupta, K., Dhawan, R., Gupta, L., et al. (2016b). Silencing of *Anopheles stephensi* heme peroxidase HPX15 activates diverse immune pathways to regulate the growth of midgut bacteria. *Front. Microbiol.* 7:1351. doi: 10.3389/fmicb.2016.01351

Kajla, M., Gupta, K., Gupta, L., and Kumar, S. (2015). A fine-tuned management between physiology and immunity maintains the gut microbiota in insects. *Biochem. Physiol.* 4:182. doi: 10.4172/2168-9652.1000182

Kajla, M., Kakani, P., Choudhury, T. P., Kumar, V., Gupta, K., Dhawan, R., et al. (2017). *Anopheles stephensi* heme peroxidase HPX15 suppresses midgut immunity to support *Plasmodium* development. *Front. Immunol.* 8:249. doi: 10.3389/fimmu.2017.00249

Kajla, M., Kakani, P., Gupta, K., Choudhury, T. P., Gupta, L., and Kumar, S. (2016a). Characterization and expression analysis of gene encoding heme peroxidase HPX15 in major Indian malaria vector *Anopheles stephensi* (Diptera: Culicidae). *Acta Trop.* 158, 107–116. doi: 10.1016/j.actatropica.2016.02.028

Kakani, P., Kajla, M., Choudhury, T. P., Gupta, L., and Kumar, S. (2019). *Anopheles stephensi* dual oxidase silencing activates the thioester-containing protein 1 pathway to suppress *Plasmodium* development. *J. Innate Immun.* 11, 496–505. doi: 10.1159/000497417

Käll, L., Krogh, A., and Sonnhammer, E. L. (2007). Advantages of combined transmembrane topology and signal peptide prediction–the Phobius web server. *Nucleic Acids Res.* 35, W429–W432.

Kelley, L. A., Mezulis, S., Yates, C. M., Wass, M. N., and Sternberg, M. J. (2015). The Phyre2 web portal for protein modelling, prediction and analysis. *Nat. protocols* 10, 845–858. doi: 10.1038/nprot.2015.053

Klebanoff, S. J. (1968). Myeloperoxidase-halide-hydrogen peroxide antibacterial system. *J. Bacteriol.* 95, 2131–2138. doi: 10.1128/jb.95.6.2131-2138.1968

Klebanoff, S. J. (2005). Myeloperoxidase: friend and foe. *J. Leukoc. Biol.* 77, 598–625. doi: 10.1189/jlb.1204697

Kumar, S., Molina-Cruz, A., Gupta, L., Rodrigues, J., and Barillas-Mury, C. (2010). A peroxidase/dual oxidase system modulates midgut epithelial immunity in *Anopheles gambiae*. *Science* 327, 1644–1648. doi: 10.1126/science.1184008

Le, Y. J., Kim, H., Chung, J. H., and Lee, Y. (2001). Testis-specific expression of an intronless gene encoding a human poly(A) polymerase. *Mol. Cells* 11, 379–385.

Letunic, I., Doerks, T., and Bork, P. (2014). SMART: recent updates, new developments and status in 2015. *Nucleic Acids Res.* 43, D257–D260.

Liu, C. H., Chen, W., Kuo, C. M., and Chen, J. C. (2004). Molecular cloning and characterisation of a cell adhesion molecule, peroxinectin from the white shrimp *Litopenaeus vannamei*. *Fish Shellfish Immunol.* 17, 13–26. doi: 10.1016/j.fsi.2003.11.002

Liu, C. H., Cheng, W., and Chen, J. C. (2005). The peroxinectin of white shrimp *Litopenaeus vannamei* is synthesised in the semi-granular and granular cells, and its transcription is up-regulated with *Vibrio alginolyticus* infection. *Fish Shellfish Immunol.* 18, 431–444. doi: 10.1016/j.fsi.2004.10.005

Livak, K. J., and Schmittgen, T. D. (2001). Analysis of relative gene expression data using real-time quantitative PCR and the 2(-Delta Delta C(T)) Method. *Methods* 25, 402–408. doi: 10.1006/meth.2001.1262

Login, F. H., Balmand, S., Vallier, A., Vincent-Monégat, C., Vigneron, A., Weiss-Gayet, M., et al. (2011). Antimicrobial peptides keep insect endosymbionts under control. *Science* 334, 362–365. doi: 10.1126/science.1209728

Luckhart, S., Vodovotz, Y., Cui, L., and Rosenberg, R. (1998). The mosquito *Anopheles stephensi* limits malaria parasite development with inducible synthesis of nitric oxide. *Proc. Natl. Acad. Sci. U.S.A.* 95, 5700–5705. doi: 10.1073/pnas.95.10.5700

Magnusson, K., Mendes, A. M., Windbichler, N., Papathanos, P. A., Nolan, T., Dottorini, T., et al. (2011). Transcription Regulation of Sex-Biased Genes during Ontogeny in the Malaria Vector *Anopheles gambiae*. *PLoS One* 6:e21572. doi: 10.1371/journal.pone.0021572

Marchler-Bauer, A., Derbyshire, M. K., Gonzales, N. R., Lu, S., Chitsaz, F., Geer, L. Y., et al. (2015). CDD: NCBI's conserved domain database. *Nucleic Acids Res.* 43, D222–D226.

Mathelier, A., Zhao, X., Zhang, A. W., Parcy, F., Worsley-Hunt, R., Arenillas, D. J., et al. (2014). JASPAR 2014: an extensively expanded and updated open-access database of transcription factor binding profiles. *Nucl. Acids Res.* 42, D142–D147.

Minard, G., Mavingui, P., and Moro, C. V. (2013). Diversity and function of bacterial microbiota in the mosquito holobiont. *Parasit Vect.* 6:146. doi: 10.1186/1756-3305-6-146

Motulsky, H. J. (1999). *Analyzing Data with GraphPad Prism*. San Diego, CA: GraphPad Software Inc.

Nishikori, K., Morioka, K., Kubo, T., and Morioka, M. (2009). Age- and morph-dependent activation of the lysosomal system and Buchnera degradation in aphid endosymbiosis. *J. Insect Physiol.* 55, 351–357. doi: 10.1016/j.jinsphys.2009.01.001

Oliveira, J. H., Gonçalves, R. L., Lara, F. A., Dias, F. A., Gandara, A. C., Menna-Barreto, R. F., et al. (2011). Blood meal-derived heme decreases ROS levels in the midgut of *Aedes aegypti* and allows proliferation of intestinal microbiota. *PLoS Pathog.* 7:e1001320. doi: 10.1371/journal.ppat.1001320

Pace, C. N., and Scholtz, J. M. (1998). A helix propensity scale based on experimental studies of peptides and proteins. *Biophys. J.* 75, 422–427. doi: 10.1016/s0006-3495(98)77529-0

Petersen, T. N., Brunak, S., von Heijne, G., and Nielsen, H. (2011). SignalP 4.0: discriminating signal peptides from transmembrane regions. *Nat. Methods* 8, 785–786. doi: 10.1038/nmeth.1701

Peterson, T. M., and Luckhart, S. (2006). A mosquito 2-Cys peroxiredoxin protects against nitrosative and oxidative stresses associated with malaria parasite infection. *Free Radic. Biol. Med.* 40, 1067–1082. doi: 10.1016/j.freeradbiomed.2005.10.059

Ramakers, C., Ruijter, J. M., Lekanne Deprez, R. H., and Moorman, A. F. (2003). Assumption-free analysis of quantitative real-time polymerase chain reaction (PCR) data. *Neurosci. Lett.* 339, 62–66. doi: 10.1016/s0304-3940(02)01423-4

Ruoslahti, E. (1996). RGD and other recognition sequences for integrins. *Annu. Rev. Cell. Dev. Biol.* 12:697e715. doi: 10.1146/annurev.cellbio.12.1.697

Saitou, N., and Nei, M. (1987). The neighbor-joining method: a new method for reconstructing phylogenetic trees. *Mol. Biol. Evol.* 4, 406–425.

Senger, K., Harris, K., and Levine, M. (2006). GATA factors participate in tissue-specific immune responses in *Drosophila* larvae. *Proc. Natl. Acad. Sci. U.S.A.* 103, 15957–15962. doi: 10.1073/pnas.0607608103

Shabalina, S. A., Ogurtsov, A. Y., Spiridonov, A. N., Novichkov, P. S., Spiridonov, N. A., and Koonin, E. V. (2010). Distinct patterns of expression and evolution of intronless and intron-containing mammalian genes. *Mol. Biol. Evol.* 27, 1745–1749. doi: 10.1093/molbev/msq086

Shanthi, S., Manju, S., Rajakumaran, P., and Vaseeharan, B. (2014). Molecular cloning of peroxinectin gene and its expression in response to peptidoglycan and *Vibrio harveyi* in Indian white shrimp *Fenneropenaeus indicus*. *Cell Commun. Adhes.* 21, 281–289. doi: 10.3109/15419061.2014.943396

Soudi, M., Zamocky, M., Jakopitsch, C., Furtmüller, P. G., and Obinger, C. (2012). Molecular evolution, structure, and function of peroxidasins. *Chem. Biodivers.* 9, 1776–1793. doi: 10.1002/cbdv.201100438

Stanke, M., Diekhans, M., Baertsch, R., and Haussler, D. (2008). Using native and syntenically mapped cDNA alignments to improve de novo gene finding. *Bioinformatics* 24, 637–644. doi: 10.1093/bioinformatics/btn013

Vizzini, A., Parrinello, D., Sanfratello, M. A., Mangano, V., Parrinello, N., and Cammarata, M. (2013). *Ciona intestinalis* peroxinectin is a novel component of the peroxidase-cyclooxygenase gene superfamily upregulated by LPS. *Dev. Comp. Immunol.* 41, 59–67. doi: 10.1016/j.dci.2013.03.015

Von Kalm, L., Crossgrove, K., Von Seggern, D., Guild, G. M., and Beckendorf, S. K. (1994). The broad-complex directly controls a tissue-specific response to the steroid hormone ecdysone at the onset of *Drosophila* metamorphosis. *EMBO J.* 13, 3505–3516. doi: 10.1002/j.1460-2075.1994.tb06657.x

Wang, Y., Gilbreath, T. M. I. I. I., Kukutla, P., Yan, G., and Xu, J. (2011). Dynamic gut microbiome across life history of the malaria mosquito *Anopheles gambiae* in Kenya. *PLoS One* 6:e24767. doi: 10.1371/journal.pone.0024767

Yang, J., Yan, R., Roy, A., Xu, D., Poisson, J., and Zhang, Y. (2015). The I-TASSER Suite: protein structure and function prediction. *Nat. Methods* 12, 7–8. doi: 10.1038/nmeth.3213

Zakovic, S., and Levashina, E. A. (2017). NF-κB-like signaling pathway REL2 in immune defenses of the malaria vector *Anopheles gambiae*. *Front. Cell Infect. Microbiol.* 7:258. doi: 10.3389/fcimb.2017.00258

Zhang, Y. (2008). I-TASSER server for protein 3D structure prediction. *BMC Bioinformatics* 9:40. doi: 10.1186/1471-2105-9-40

Zhu, J., Chen, L., and Raikhel, A. S. (2007). Distinct roles of broad isoforms in regulation of the 20-hydroxyecdysone effector gene, Vitellogenin, in the mosquito *Aedes aegypti*. *Mol. Cell. Endocrinol.* 267, 97–105. doi: 10.1016/j.mce.2007.01.006